processes

MDPI

Communication

Microbial Anode-Driven Electro-Fermentation for Succinate Production

Jingjing Wang and Wenqiao Yuan *

Department of Biological and Agricultural Engineering, North Carolina State University, Raleigh, NC 27695, USA
* Correspondence: wyuan2@ncsu.edu

Abstract

This study demonstrates a proof-of-concept microbial electrochemical system (MES) that integrates a *Geobacter sulfurreducens* anodic biofilm with *Actinobacillus succinogenes* cathodic electro-fermentation. The anode, poised at 0 V versus Ag/AgCl, supported extracellular electron transfer from acetate oxidation, yielding a coulombic efficiency of up to 72.9%. When the cathode was switched from an abiotic ferricyanide sink to *A. succinogenes* medium containing neutral red, current increased sharply, reflecting mediator-assisted electron transfer. Cathodic metabolism showed a redirection in flux: succinate selectivity improved by 9.9%, increasing from 42.9% to 52.8% of input carbon, while formate and acetate decreased by 7.8% and 3.0%, respectively, without loss in overall carbon recovery. This improvement in succinate selectivity is industrially relevant in that it not only increases succinate yield but also lowers separation costs due to lower byproducts (formate and acetate). These results reveal that a poised *G. sulfurreducens* anode can sustain sufficient current to influence *A. succinogenes* product distribution, supporting the feasibility of biologically integrated MES-electro-fermentation. Potential hydrogen evolution, which could possibly contribute to increased succinate selectivity, was a thermodynamic possibility rather than a confirmed pathway. Future work was proposed to resolve electron partitioning, mediator kinetics, and cross-feeding interactions.

Keywords: microbial electrochemical system (MES); *Geobacter sulfurreducens*; *Actinobacillus succinogenes*; electro-fermentation; succinic acid; succinate

1. Introduction

Microbial electrochemical systems (MESs) are an emerging platform technology that combines microbial metabolism with electrochemistry, materials science, and engineering. They offer new opportunities for energy recovery and bioproduction from renewable resources [1]. In typical designs, the anode hosts electroactive microorganisms that oxidize organic substrates and release electrons, while the cathode consumes electrons to drive reductive reactions that can support bioproduct formation [2].

Among many electroactive microorganisms, *Geobacter sulfurreducens* is a Gram-negative, strictly anaerobic, dissimilatory metal-reducing bacterium that is widely used as a model in MESs. It is well known for oxidizing acetate, lactate, and formate and coupling this metabolism to extracellular electron acceptors such as ferric iron (Fe^{3+}) and Manganese oxides [3,4]. In addition to metals, the electrode can also serve as an electron acceptor, making *G. sulfurreducens* an effective biocatalyst for anodic electricity generation [5]. To study anodic electricity generation under well-defined conditions and minimize cathodic limitations, many studies employ poised anode potentials. For example, Bond and Lovley

Check for updates

Academic Editors: Francesca Raganati and Alessandra Procentese

Received: 19 November 2025
Revised: 21 January 2026
Accepted: 28 January 2026
Published: 1 February 2026

Copyright: © 2026 by the authors. Licensee MDPI, Basel, Switzerland. This article is an open access article distributed under the terms and conditions of the Creative Commons Attribution (CC BY) license.

compared uncontrolled and poised anode operations and found that electricity production was directly linked to the growth of *G. sulfurreducens* on the electrode, with maximum current densities obtained when the anode was held at +0.2 V vs. Ag/AgCl [6].

The reliance of MESs on abiotic cathodes remains a major limitation. In most cases, electrons released at the anode are ultimately consumed by oxygen or ferricyanide to complete the circuit. Oxygen reduction is convenient and sustainable but kinetically sluggish and dependent on costly catalysts. At neutral pH, the theoretical potential of the O_2/H_2O couple is +0.805 V versus SHE, yet the measured potential of oxygen cathodes is typically closer to +0.2 V. This large overpotential illustrates that even a thermodynamically favorable process can be severely constrained by kinetic barriers under practical conditions [7]. Even platinum-based cathodes can enhance oxygen reduction, but their susceptibility to poisoning and high cost limit practical application [8]. Another common electron acceptor in cathode is ferricyanide, which offers favorable kinetics and a stable potential for laboratory studies, but it is depleted stoichiometrically and reduced to ferrocyanide, rendering it unsuitable for practical use [9].

Biocathodes offer an alternative to abiotic cathodes by channeling electrons into microbial metabolism rather than wasting them on non-productive sinks. The feasibility of coupling acetate oxidation at the anode with microbial activity at the cathode has been demonstrated in several studies. For example, Clauwaert et al. combined an acetate-oxidizing bioanode with an oxygen-reducing biocathode, where cathodic microorganisms replaced platinum as biocatalysts for oxygen reduction [10]. Similarly, Rabaey et al. showed that electrons released from acetate oxidation at the anode could be transferred through the external circuit and accepted by microbial communities at the cathode, which catalyzed oxygen reduction [11]. Another study showed that electrons generated from acetate oxidation at the anode were directed to a biocathode, where they were accepted by microorganisms and coupled to bicarbonate reduction, enabling simultaneous electricity generation and CO_2 fixation [12]. Together, these studies illustrated that anodic electrons could be integrated into microbial metabolism at the cathode, expanding the functional scope of microbial electrochemical systems.

In parallel, *A. succinogenes* is a natural succinate producer whose metabolism depends on intracellular redox balance. It is a Gram-negative, facultative anaerobic bacterium [13]. Supplying external reducing power has been shown to enhance succinate yields while suppressing competing byproducts such as formate and acetate [13]. These systems are referred to as microbial electrolysis cells, electro-fermentation, or bioelectrochemical systems, but the underlying principle is the same: reducing power is delivered through abiotic anodes connected to potentiostats or DC power supplies. Cathode-derived electrons, often mediated by shuttles such as neutral red, shift metabolic fluxes and improve succinate selectivity, but they require continuous external energy input [14–17]. A more sustainable alternative is to replace abiotic anodes with bioanodes that generate current through microbial metabolism, thereby enabling *A. succinogenes* to function as a biocathode in a fully biological electron flow.

Building on this framework, the present study demonstrates a proof-of-concept that integrates a *G. sulfurreducens* bioanode with an *A. succinogenes* biocathode. In previous MES or electro-fermentation studies, systems typically prioritized either electricity generation using a bioanode with a non-productive cathodic reaction, or product formation at the cathode supported by an external power supply with the anodic reaction effectively wasted. As a result, electron flow was only partially utilized. The key motivation of the present work was to evaluate whether a microbial bioanode and a fermentative biocathode can be directly integrated so that both anodic and cathodic metabolisms are productive. In such a configuration, biocathodic byproducts (formate and acetate) may serve as substrates for the

bioanode, while electrons generated at the bioanode can be utilized to enhance succinate selectivity, thereby reducing external inputs and improving overall system efficiency. The objective was to assess the feasibility of this integration. Anodic performance was evaluated in terms of current generation and stability under poised potentials, while cathodic performance was assessed by product yields, carbon distribution, and electron recovery. This work provides a step toward future microbial fuel cells that can fully support cathodic electro-fermentation for bioproduct formation.

2. Materials and Methods

2.1. Microorganisms and Cultivation

Geobacter sulfurreducens (ATCC 51573) and *Actinobacillus succinogenes* (ATCC 55618) were purchased from the American Type Culture Collection (ATCC, Manassas, VA, USA), and both strains were revived according to ATCC instructions. *G. sulfurreducens* was cultivated using acetate (20 mM) as the electron donor and fumarate (40 mM) as the electron acceptor under strictly anaerobic conditions at 30 °C. Cultures were grown to mid-log phase and inoculated at an OD_{600} of 0.1–0.2. *A. succinogenes* was cultivated in a medium containing xylose (15 g/L) and $NaHCO_3$ (10 g/L) as the CO_2 source at 37 °C, and seed cultures were harvested at mid-log phase for reactor inoculation.

2.2. Construction of MES Reactor

A dual-chamber system was constructed using two glass bottles connected by 40-mm-diameter glass flanges (Adams & Chittenden Scientific Glass, Berkeley, CA, USA), secured with chemical-resistant seals and wraparound knuckle clamps. Each chamber had a total volume of 330 ± 5 mL, consisting of a 270 mL liquid working volume (including the electrode) and a 60 mL headspace. The two chambers were separated by a proton exchange membrane (PFSA D 170-U, Fuel Cell Store, Bryan, TX, USA). Graphite felt electrodes (3 × 4 × 0.8 cm; AvCarb, Lowell, MA, USA) served as working and counter electrodes. An Ag/AgCl reference electrode (3 M NaCl, +0.205 V vs. SHE) was placed in the anode chamber, and the anode potential was poised at 0 V vs. Ag/AgCl using a potentiostat (EmStat4X; BASi, West Lafayette, IN, USA). Reactors were maintained at 30 °C in an incubator, with continuous mixing at 130 rpm using magnetic stir bars.

2.3. Operation of MES with G. sulfurreducens

The anode biofilm was established using a three-phase cultivation strategy. In the first phase, *G. sulfurreducens* was grown in the anode chamber with fumarate (40 mM) as the terminal electron acceptor and acetate (20 mM) as the electron donor. An actively growing culture (50 mL) was inoculated into 200 mL of this medium. In the second phase, the anode was poised at 0 V vs. Ag/AgCl to promote electron transfer and biofilm formation. In the third phase, the anolyte was replaced with fresh medium lacking fumarate, forcing *G. sulfurreducens* to use the anode as the sole terminal electron acceptor for current generation. All medium exchanges were performed under anoxic conditions by sparging with N_2/CO_2 (80:20). The anode medium contained the following chemicals: KH_2PO_4 (2.829 g/L), K_2HPO_4 (5.087 g/L), sodium acetate (1.64 g/L), NH_4Cl (1.5 g/L), $MgCl_2 \cdot 6H_2O$ (0.1 g/L), $CaCl_2 \cdot 2H_2O$ (0.1 g/L), KCl (0.1 g/L), Wolfe's vitamins (10 mL/L), and Wolfe's minerals (10 mL/L). The cathode medium consisted of KH_2PO_4 (5.07 g/L), K_2HPO_4 (10.928 g/L), and potassium ferricyanide ($K_3[Fe(CN)_6]$) at a final concentration of 50 mM.

2.4. Integration of MES and Cathodic Electro-Fermentation

Once the *G. sulfurreducens* anode biofilm achieved stable growth under poised potential, the system was integrated with cathodic electro-fermentation. Prior to integration,

the anode chamber was replenished with fresh anode medium to sustain biofilm activity, while the cathode chamber medium was replaced with *A. succinogenes* medium, which contained: 100 mM phosphate buffer (pH 7.0), 5 g/L yeast extract, 15 g/L xylose, and 10 g/L $NaHCO_3$. Neutral red was added to the catholyte as a redox mediator at a final concentration of 0.1 mM after sterile filtration through a 0.22 µm membrane filter. Media transfers were conducted under anoxic conditions using N_2/CO_2 sparging and a peristaltic pump, following the protocol described by O'Brien and Malvankar [18]. The cathode chamber was then inoculated with *A. succinogenes* to an initial optical density (OD600) of 0.1 to establish active growth at the start of integration. The overall configuration of the integrated MES-cathodic electro-fermentation system is illustrated in Figure 1.

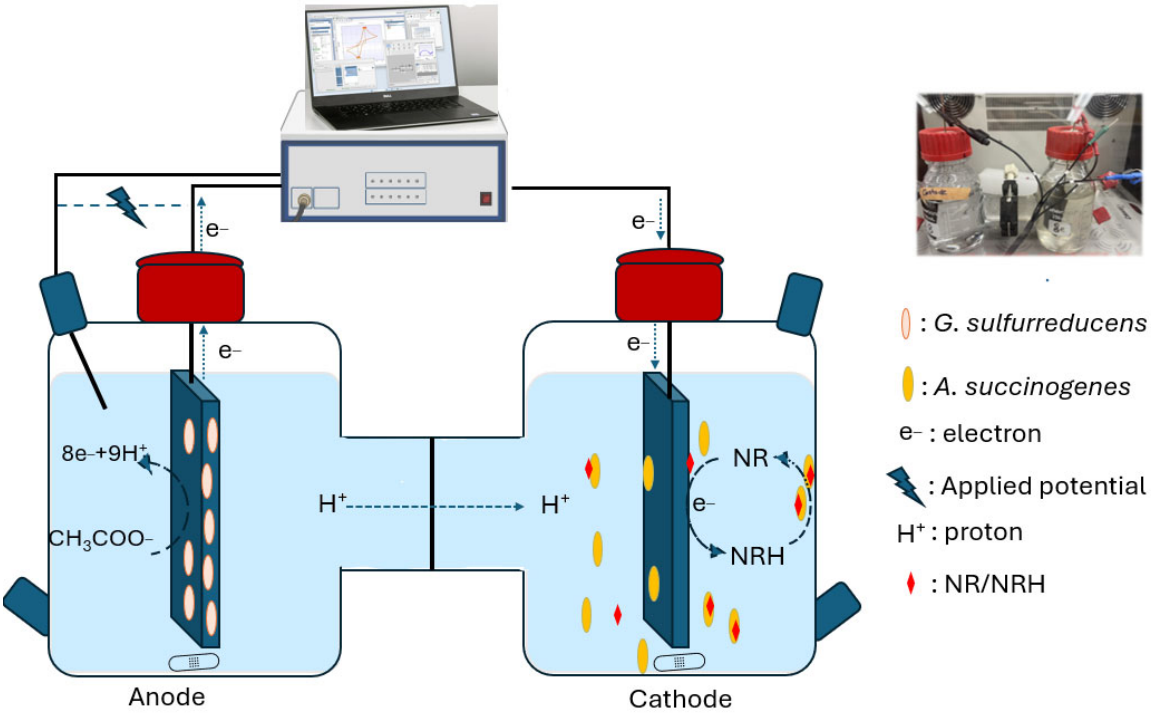


Figure 1. Schematic representation of the integrated MES–cathodic electro-fermentation system.

2.5. Bioelectrochemical Analysis

Bioelectrochemical performance was monitored by chronoamperometry (CA). CA was used to quantify electron transfer to the anode and to track biofilm growth, substrate utilization, and system stability over time. Anode potential (0 V vs. Ag/AgCl) and whole-cell potential were recorded continuously throughout the experiments.

2.6. Metabolite Analysis

Planktonic growth was monitored by OD600 using a microplate reader (BioTek Instruments, Winooski, VT, USA). Acetate and succinate were quantified by high-performance liquid chromatography (HPLC; Shimadzu Corporation, Kyoto, Japan) equipped with UV–Vis and refractive index detectors. Separations were performed on an Aminex HPX-87H column (300 × 7.8 mm; Bio-Rad, Hercules, CA, USA) maintained at 50 °C, using 0.005 M H_2SO_4 as the mobile phase at 0.5 mL/min, with detector temperature set at 40 °C.

2.7. Coulombic Efficiency and Carbon Flux Calculations

Coulombic efficiency (CE) was calculated as the ratio of electrons recovered as electrical current to the theoretical electrons released from substrate oxidation:

$$CE\% = \frac{Q_{measured}}{Q_{theoretical}} \times 100 \quad (1)$$

$$Q_{measured} = \int I(t)dt \quad (2)$$

$$Q_{theoretical} = n_e \times F \times \Delta S \quad (3)$$

where $Q_{measured}$ is the total charge (C) obtained by integrating current over time, and $Q_{theoretical}$ is the charge equivalent of electrons released from acetate oxidation. Acetate oxidation follows the reaction: $CH_3COO^- + 2H_2O \rightarrow 2CO_2 + 7H^+ + 8e^-$, yielding 8 mol e^- per mol acetate consumed. The corresponding charge was calculated from acetate concentration changes using Faraday's constant (F = 96,485 C-mol^{-1} e^-).

Carbon flux distributions were calculated as the fraction of input carbon (C-mol) recovered in each product. Input carbon was defined as five C-mol per mole of xylose consumed plus one C-mol per mole of succinate formed (accounting for bicarbonate incorporation). For each metabolite, the number of carbon per mole was multiplied by its molar concentration to obtain carbon equivalents (C-mol L^{-1}). The percentage contribution of each product was then expressed as

$$Carbon\ flux\ (\%) = \frac{C_{product}}{C_{xylose} + C_{bicarbonate}} * 100 \quad (4)$$

where $C_{product}$ is the carbon equivalents (C-mol) recovered in succinate, formate, or acetate, and the denominator represents the total input carbon equivalents.

3. Results and Discussion

3.1. Anode Electrochemical Performance

Current generation at the poised anode is shown in Figure 2. The chronoamperometric profile suggests distinct growth phases of *G. sulfurreducens* on the anode and a clear response to medium replacement. From 0 to 25 h, the gradual increase in current reflects cell attachment and early biofilm development, with progressively enhanced electron transfer to the anode. Between 25 and 38 h, the current reached a plateau and then slightly declined, indicating the onset of electron donor or nutrient limitation, or the accumulation of inhibitory byproducts. At around 38 h, medium replacement results in an immediate increase in current, indicating that electron transfer was limited by medium conditions rather than loss of biofilm activity. Following replacement, the current continued to rise and reached a maximum at 55–60 h, reflecting a period of enhanced biofilm activity and electron transfer efficiency. After 60 h, the current gradually declines through 120 h, consistent with renewed nutrient depletion, biofilm maturation, or increasing mass-transfer limitations.

In the initial phase with a cathode containing ferricyanide buffer as the electron acceptor (0 to 38 h), the current increased to 4 mA before declining. During this period, acetate consumption in the anode reached 1.15 mmol, corresponding to a theoretical electron release of 885 C. Of these electrons, 428.5 C were recovered as current at the anode, while partial reduction of residual fumarate to succinate accounted for 88 C. The combined sinks yielded a coulombic efficiency of 53.8%. These results are summarized in Table 1. The decline in current at 38 h suggested nutrient limitation in the anode or depletion/saturation of the cathodic ferricyanide buffer.

After medium exchange, the reactor was operated as an integrated MES-cathodic electro-fermentation system. The current increased sharply to 8 mA and then declined gradually. In the cathode, NR was reduced to NRH at the poised potential, providing an effective mediator for electron transfer and sustaining the elevated current. At the anode,

acetate was oxidized by *G. sulfurreducens*, and the released electrons were delivered to the electrode through extracellular electron transfer (EET). Holding the anode at 0 V vs. Ag/AgCl imposed a positive driving force relative to the biofilm redox midpoint (−0.36 V vs. Ag/AgCl), which thermodynamically promoted acetate oxidation and kinetically supported stable current generation. This behavior is consistent with established EET mechanisms in *Geobacter* spp. [19].

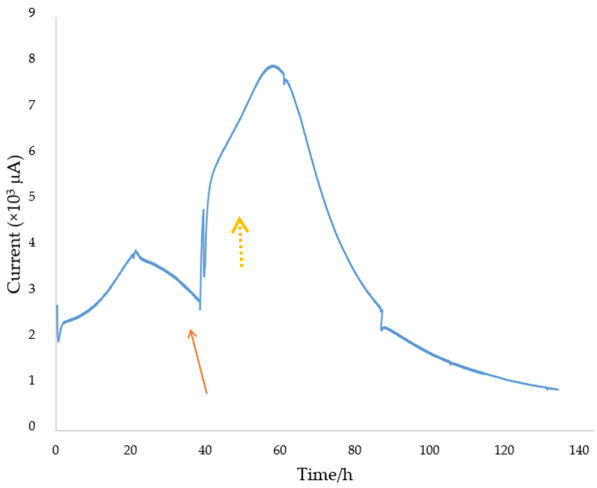


Figure 2. Chronoamperometric current profile of the system at an anode potential of 0 V vs. Ag/AgCl over 134 h. During the initial 0 to 38 h, current rose and then declined, reflecting the first growth phase of *G. sulfurreducens* on acetate with the anode as the sole electron acceptor, while the cathode was abiotic. At 38 h (medium replacement point shown as the yellow arrow), the anode chamber was replenished with fresh growth medium, and the cathode chamber was replaced with *A. succinogenes* medium supplemented with neutral red. Following this replacement, current increased sharply to a maximum before declining to a low and stable level, indicating enhanced electron transfer during active growth followed by a gradual loss of activity.

Table 1. Summary of AA concentration, electron release by AA oxidation, and coulombic efficiency (CE). $Q_{electrode}$ denotes the cumulative charge delivered to the electrode (Coulombs), calculated by integrating current recorded at one-minute intervals over a 134 h operation from a representative run. Q_{AA} represents electron equivalents recovered in AA. Substrate concentrations are expressed as mean ± standard deviation.

Time (h)	**0**	**38**		**39**	**136**
AA (mM)	19.73 ± 0.29	15.48 ± 0.18	medium replacement	19.22 ± 0.24	11.06 ± 0.17
Q_{AA} (C)	885			1698	
$Q_{electrode}$ (C)	429			1237	
CE (%)	53.8			72.9	

During the second phase (39 to 134 h), total acetate consumption was 2.20 mmol (19.22–11.06 mM in 270 mL media), equivalent to 1698 C. The integrated anodic current accounted for 1237 C, yielding a coulombic efficiency of 72.9% (Table 1). These results demonstrate a more efficient electron recovery compared to the abiotic ferricyanide cathode phase.

3.2. Cathode Electrochemical Performance

The cathode chamber was switched to *A. succinogenes* medium containing NR at 39 h. Electrons delivered through the circuit reduced NR at the cathode to NRH, which subsequently provided reducing equivalents to the cells and supported the reductive metabolism leading to succinate formation improvement. In fermentations with *A. succinogenes*, apply-

ing an external potential with NR as the mediator has been shown to enhance succinate selectivity by improving intracellular redox balance [20].

Compared to the control without a poised potential, xylose consumption under poised conditions decreased by 9.8%, from 12.12 to 10.93 g/L (Table 2). Succinate concentration increased by 14.3%, rising from 5.72 to 6.54 g/L. Formate decreased by 53.2%, from 3.29 to 1.54 g/L, and acetate decreased by 18.5%, from 3.36 to 2.74 g/L. The increase in succinate titer was consistent with the additional reducing equivalents supplied by the bioanode, whereas the decrease in xylose consumption was less clear. One possible explanation is that improved redox balance under electrochemical coupling reduced the need for substrate oxidation to maintain redox balance. However, this was not confirmed in the present study, and further measurements of substrate uptake, biomass growth, and local cathodic conditions would be needed to clarify this effect.

Table 2. Xylose consumption and product titers of SA, FA, and AA under control and anode-poised conditions. Changes are expressed as percent differences relative to the control, with positive values indicating an increase and negative values indicating a decrease under poised conditions. Measured values are expressed as mean ± standard deviation. Values are reported as mean ± standard deviation (n = 2). Different letters within the same row indicate a significant difference between the control and anode-poised conditions ($p < 0.05$, two-tailed Welch's t-test); identical letters indicate no significant difference.

	Control (g/L)	Anode Poised (g/L)	Change
Xylose consumed	12.12 ± 0.76 [a]	10.93 ± 0.65 [a]	−9.83%
SA titer	5.72 ± 0.24 [a]	6.54 ± 0.19 [a]	+14.3%
FA titer	3.29 ± 0.07 [a]	1.54 ± 0.04 [b]	−53.2%
AA titer	3.36 ± 0.02 [a]	2.74 ± 0.05 [b]	−18.5%

On a molar yield basis, succinate increased by 26.8%, from 0.600 to 0.761 mol/mol, while formate decreased by 48.1%, from 0.884 to 0.459 mol/mol, and acetate decreased by 9.5%, from 0.693 to 0.627 mol/mol. These results are summarized in Table 3. Carbon fluxes were expressed as percentages of input carbon, defined as five carbons from xylose plus one bicarbonate carbon per mole of succinate. In the control, succinate accounted for 42.9%, formate for 15.8%, and acetate for 24.8% of input carbon (sum 83.4%). Under poised condition, succinate increased to 52.8%, while formate and acetate decreased to 8.0% and 21.8%, respectively (sum 82.6%). Compared with the control, 9.9% of input carbon was redirected toward succinate, largely at the expense of formate (−7.8%) and acetate (−3.0%). Overall carbon recovery remained essentially unchanged.

Table 3. Molar yields (mol product per mol xylose consumed) and corresponding carbon flux distributions of succinate (SA), formate (FA), and acetate (AA) under control and anode-poised conditions. Measured values are expressed as mean ± standard deviation. Different letters within the same column indicate a significant difference between the control and anode-poised conditions ($p < 0.05$, two-tailed Welch's t-test); identical letters indicate no significant difference.

	SA	FA	AA
control (mol/mol)	0.60 ± 0.02 [a]	0.88 ± 0.03 [a]	0.69 ± 0.03 [a]
Anode poised (mol/mol)	0.76 ± 0.01 [b]	0.46 ± 0.01 [b]	0.63 ± 0.02 [a]
Carbon flux (%)-control	42.9%	15.8%	24.8%
Carbon flux (%)-anode poised	52.8%	8.0%	21.8%

Before the switch at 39 h, ferricyanide in the catholyte functioned as the terminal electron acceptor. After switching, neutral red served as the electron acceptor and primary mediator. Replacing ferricyanide with neutral red as the electron acceptor changed cathode

behavior. Ferricyanide, a fast electron acceptor with a redox potential of approximately +0.36 V vs. SHE, maintained a relatively less negative cathode potential and higher current. In contrast, neutral red, with a midpoint redox potential of approximately −0.525 V vs. Ag/AgCl at neutral pH [21], showed slower redox kinetics and required a more negative cathode potential to sustain electron transfer. Under these conditions, neutral red can reversibly cycle between reduced and oxidized forms, accepting electrons at the cathode and transferring them to *A. succinogenes*, thereby functioning as a reusable electron shuttle rather than being consumed. With the anode held at 0 V vs. Ag/AgCl, the potentiostat adjusted the cathode potential to sustain current. Based on the logged cell voltage, the inferred cathode potential was more negative than −0.525 V, creating a favorable thermodynamic and kinetic driving force for NR reduction. This sufficiently negative potential accelerated NR to NRH conversion and coincided with the sharp increase in current.

As the *A. succinogenes* population increased, a larger fraction of cells participated in NR cycling. More cells interacting with NRH resulted in back-and-forth conversion between NR and NRH, which strengthened the electron shuttle between the electrode and the culture. This intensified NR cycling sustained higher electron flow through the circuit and was reflected in elevated anodic currents. The enhanced electron flux increased intracellular reducing equivalents, shifting metabolism toward pathways favoring more reduced products. Succinate formation was therefore increased, while formate and acetate productions were suppressed. This trend aligns with previous studies showing that applying a cathodic potential directly to the cathode enhanced succinate production and suppressed formate and acetate [13]. In the current system, however, the effective cathodic potential was imposed indirectly by the poised anode rather than direct cathode polarization.

By 48 h after *A. succinogenes* inoculation (87 h total runtime), xylose in the cathode medium was depleted. With substrate exhausted, *A. succinogenes* activity declined, NRH cycling ceased, and the current returned toward baseline levels. This transition was visually confirmed by the loss of neutral red coloration, as the catholyte shifted from red (NR) to yellow, matching the spent medium in the control.

3.3. Consideration of Possible Hydrogen Evolution

In addition to NR-mediated electron transfer, the large cell potential, which may result in a highly negative cathode potential, raises the possibility that a fraction of the electron flux was diverted toward hydrogen evolution reaction (HER). The cathode potential was not measured directly but inferred from the potentiostat output. As shown in Figure 3, the potentiostat recorded the cell potential as the difference between the working and counter electrode potentials. With the anode (working electrode) maintained at 0 V vs. Ag/AgCl, the cathode potential was estimated as the negative of the measured cell potential. This back-calculated value represents a conservative, most-negative bound because it does not account for ohmic resistance or electrode polarization. The true interfacial cathode potential was therefore less negative, but its exact value could not be known without a reference electrode placed in the cathode compartment.

From a thermodynamic standpoint, hydrogen evolution was feasible under these assumptions. The H_2/H^+ redox couple lies near −0.62 V vs. Ag/AgCl at pH 7, whereas the inferred cathode potential approached −1.8 V, well within the range required for abiotic H_2 formation. However, the cathode was composed of graphite felt, a material with intrinsically poor catalytic activity for hydrogen evolution. This imposes a substantial kinetic barrier, with HER on bare graphite typically initiating only around −1.0 V vs. Ag/AgCl and becoming appreciable only at more negative potentials [22,23]. Considering both the sluggish kinetics of graphite felt and the uncertainty in the actual interfacial potential, hydrogen evolution in this system is best regarded as a thermodynamic possibility

rather than a confirmed pathway. Future studies should include direct H_2 detection (e.g., headspace gas chromatography or in situ microsensors) and the placement of a reference electrode in the cathode chamber to better resolve cathodic potentials and quantify HER contributions.

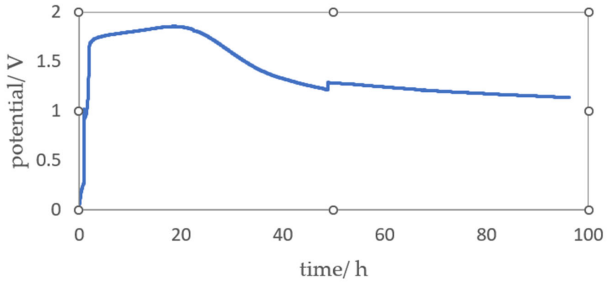


Figure 3. Cell potential profile over 96 h with the anode poised at 0 V vs. Ag/AgCl. The potentiostat recorded the cell potential as the difference between working and counter electrodes. Recording began immediately after medium replacement in both anode and cathode chambers.

4. Conclusions

This work demonstrated that integrating a *G. sulfurreducens* bioanode with an *A. succinogenes* biocathode can establish a biologically driven electron flow that reshapes metabolic output. Unlike conventional MES designs that rely on abiotic cathodes, this system channels anodic electrons into microbial metabolism, increasing succinate selectivity from 42.9% to 52.8% of carbon input while decreasing FA and AA yields, with overall carbon recovery essentially unchanged.

5. Future Work

For the first time, this study demonstrated the feasibility of coupling a *G. sulfurreducens* bioanode with an *A. succinogenes* biocathode. However, several limitations remain. First, cathode potentials were not directly measured but inferred from potentiostat cell voltages. These values represent conservative, most-negative bounds because ohmic resistance and electrode polarization were not corrected. Future work should incorporate a reference electrode in the cathode chamber to directly measure the interfacial potential. Such measurements are essential for understanding how the cathode responds to the imposed anode potential and for clarifying its role in electron allocation, metabolite redistribution, and possible hydrogen evolution.

Second, hydrogen evolution was considered only as a thermodynamic possibility under the poised-anode condition. Although the inferred cathodic potentials reached strongly negative values that could, in principle, support hydrogen evolution, hydrogen production was not directly measured in this study. In addition, the absence of a cathodic reference electrode prevented the determination of the true interfacial cathode potential after accounting for ohmic losses and polarization effects. The use of graphite felt as the cathode material further increased uncertainty, as its relatively poor catalytic activity toward hydrogen evolution might suppress detectable H_2 formation even when it was thermodynamically feasible. As a result, the fraction of current potentially diverted to hydrogen evolution could not be quantified and may range from negligible to non-negligible under the present conditions. Resolving this uncertainty will require direct headspace gas analysis, in situ hydrogen sensing, and accurate cathode potential measurements in future studies to close the electron balance and clarify the role of hydrogen in the integrated system.

Third, a useful extension of this study would be to evaluate whether the integrated MES can operate spontaneously without an externally poised potential. The main factors limiting spontaneous operation under the present conditions include: (i) insufficient overall

cell voltage and energy losses associated with electrode overpotentials and internal resistance, which require external potential control to sustain current; (ii) cathodic limitations related to electron uptake kinetics, mediator performance, and possible hydrogen evolution, as well as membrane and solution ohmic losses; and (iii) the need for a sufficiently mature anodic biofilm to generate stable current. In addition, the timing of cathode inoculation is critical, as anodic current generation, cathodic microbial growth, and electron consumption must be well matched to maintain a balanced system operation. Optimizing these parameters will be essential to establish a self-sustaining system.

Author Contributions: Conceptualization, J.W. and W.Y.; methodology, J.W.; formal analysis, J.W.; writing—original draft preparation, J.W.; writing—review and editing, W.Y.; funding acquisition, W.Y. All authors have read and agreed to the published version of the manuscript.

Funding: This research was funded by North Carolina Department of Agriculture and Consumer Services, grant number 22-035-4001; the US Department of Agriculture National Institute of Food and Agriculture, Hatch Project NC 02866; the US Department of Agriculture National Institute of Food and Agriculture, Multistate Project S1075.

Data Availability Statement: The original contributions presented in this study are included in the article. Further inquiries can be directed to the corresponding author.

Conflicts of Interest: The authors declare no conflicts of interest.

References

1. Wang, H.; Ren, Z.J. A comprehensive review of microbial electrochemical systems as a platform technology. *Biotechnol. Adv.* **2013**, *31*, 1796–1807. [CrossRef]
2. Kumar, R.; Singh, L.; Zularisam, A.W. *Microbial Fuel Cells: Types and Applications. Waste Biomass Management—A Holistic Approach*; Springer: Berlin/Heidelberg, Germany, 2017; pp. 367–384. [CrossRef]
3. Marsili, E.; Rollefson, J.B.; Baron, D.B.; Hozalski, R.M.; Bond, D.R. Microbial Biofilm Voltammetry: Direct Electrochemical Characterization of Catalytic Electrode-Attached Biofilms. *Appl. Environ. Microbiol.* **2008**, *74*, 7329–7337. [CrossRef]
4. Caccavo, F.; Lonergan, D.J.; Lovley, D.R.; Davis, M.; Stolz, J.F.; McInerney, M.J. *Geobacter sulfurreducens* sp. nov., a hydrogen- and acetate-oxidizing dissimilatory metal-reducing microorganism. *Appl. Environ. Microbiol.* **1994**, *60*, 3752–3759. [CrossRef]
5. Scarabotti, F.; Rago, L.; Bühler, K.; Harnisch, F. The electrode potential determines the yield coefficients of early-stage *Geobacter sulfurreducens* biofilm anodes. *Bioelectrochemistry* **2021**, *140*, 107752. [CrossRef]
6. Bond, D.R.; Lovley, D.R. Electricity Production by *Geobacter sulfurreducens* Attached to Electrodes. *Appl. Environ. Microbiol.* **2003**, *69*, 1548–1555. [CrossRef] [PubMed]
7. Logan, B.E.; Hamelers, B.; Rozendal, R.; Schröder, U.; Keller, J.; Freguia, S.; Aelterman, P.; Verstraete, W.; Rabaey, K. Microbial Fuel Cells: Methodology and Technology. *Environ. Sci. Technol.* **2006**, *40*, 5181–5192. [CrossRef] [PubMed]
8. Ojha, R.; Dash, J.; Satpathy, S.S.; Ojha, P.C.; Pradhan, D. A brief review on factors affecting the performance of microbial fuel cell and integration of artificial intelligence. *Discov. Sustain.* **2025**, *6*, 702. [CrossRef]
9. Lawson, K.; Rossi, R.; Regan, J.M.; Logan, B.E. Impact of cathodic electron acceptor on microbial fuel cell internal resistance. *Bioresour. Technol.* **2020**, *316*, 123919. [CrossRef] [PubMed]
10. Clauwaert, P.; van der Ha, D.; Boon, N.; Verbeken, K.; Verhaege, M.; Rabaey, K.; Verstraete, W. Open Air Biocathode Enables Effective Electricity Generation with Microbial Fuel Cells. *Environ. Sci. Technol.* **2007**, *41*, 7564–7569. [CrossRef]
11. Rabaey, K.; Read, S.T.; Clauwaert, P.; Freguia, S.; Bond, P.L.; Blackall, L.L.; Keller, J. Cathodic oxygen reduction catalyzed by bacteria in microbial fuel cells. *ISME J.* **2008**, *2*, 519–527. [CrossRef]
12. Cao, X.; Huang, X.; Liang, P.; Boon, N.; Fan, M.; Zhang, L.; Zhang, X. A completely anoxic microbial fuel cell using a photo-biocathode for cathodic carbon dioxide reduction. *Energy Environ. Sci.* **2009**, *2*, 498–501. [CrossRef]
13. Salma, A.; Djelal, H.; Abdallah, R.; Fourcade, F.; Amrane, A. Well Knowledge of the Physiology of *Actinobacillus succinogenes* to Improve Succinic Acid Production. *Appl. Microbiol.* **2021**, *1*, 304–328. [CrossRef]
14. Zhao, Y.; Cao, W.; Wang, Z.; Zhang, B.; Chen, K.; Ouyang, P. Enhanced succinic acid production from corncob hydrolysate by microbial electrolysis cells. *Bioresour. Technol.* **2016**, *202*, 152–157. [CrossRef]
15. Hengsbach, J.N.; Cwienczek, M.; Haffelder, J.; Tippkötter, N.; Ulber, R. *Actinobacillus succinogenes* in bioelectrochemical systems—Comparative study of redox mediators. *Electrochem. Commun.* **2025**, *179*, 108003. [CrossRef]

16. Pateraki, C.; Magdalinou, E.; Skliros, D.; Flemetakis, E.; Rabaey, K.; Koutinas, A. Transcriptional regulation in key metabolic pathways of *Actinobacillus succinogenes* in the presence of electricity. *Bioelectrochemistry* **2023**, *151*, 108376. [CrossRef]
17. Tix, J.; Hengsbach, J.-N.; Bode, J.; Pedraza, F.; Willer, J.; Park, S.J.; Reardon, K.F.; Ulber, R.; Tippkötter, N. *Actinobacillus succinogenes* in Bioelectrochemical Systems: Influence of Electric Potentials and Carbon Fabric Electrodes on Fermentation Performance. *Microorganisms* **2025**, *13*, 1720. [CrossRef] [PubMed]
18. Wang, Z.; Li, H.; Feng, J.; Zhang, A.; Ying, H.; He, X.; Jiang, M.; Chen, K.; Ouyang, P. Enhanced succinic acid production from polyacrylamide-pretreated cane molasses in microbial electrolysis cells. *J. Chem. Technol. Biotechnol.* **2018**, *93*, 855–860. [CrossRef]
19. O'Brien, J.P.; Malvankar, N.S. A Simple and Low-Cost Procedure for Growing *Geobacter sulfurreducens* Cell Cultures and Biofilms in Bioelectrochemical Systems. *Curr. Protoc. Microbiol.* **2016**, *43*, A.4K.1–A.4K.27. [CrossRef]
20. Kato, S. Influence of Anode Potentials on Current Generation and Extracellular Electron Transfer Paths of Geobacter Species. *Int. J. Mol. Sci.* **2017**, *18*, 108. [CrossRef]
21. Tix, J.; Gotthardt, L.; Bode, J.; Karabacak, B.; Nordmann, J.; Hengsbach, J.-N.; Ulber, R.; Tippkötter, N. Enhancement of Succinic Acid Production by *Actinobacillus succinogenes* in an Electro-Bioreactor. *Fermentation* **2024**, *10*, 504. [CrossRef]
22. Zani, A.C.B.; de Souza, J.C.; de Andrade, A.R.; Reginatto, V. Neutral Red Film Augments Extracellular Electron Transfer Performed by Clostridium pasteurianum DSM 525. *Fermentation* **2024**, *10*, 497. [CrossRef]
23. Izadi, P.; Fontmorin, J.M.; Godain, A.; Yu, E.H.; Head, I.M. Parameters influencing the development of highly conductive and efficient biofilm during microbial electrosynthesis: The importance of applied potential and inorganic carbon source. *npj Biofilms Microbiomes* **2020**, *6*, 40. [CrossRef] [PubMed]

Disclaimer/Publisher's Note: The statements, opinions and data contained in all publications are solely those of the individual author(s) and contributor(s) and not of MDPI and/or the editor(s). MDPI and/or the editor(s) disclaim responsibility for any injury to people or property resulting from any ideas, methods, instructions or products referred to in the content.